Semaphorin 3fa Controls Ocular Vascularization From the Embryo Through to the Adult

Rami Halabi,[1,3,4] Charlene Watterston,[2] Carrie Lynn Hehr,[3–5] Risa Mori-Kreiner,[1,3,4] Sarah J. Childs,[2,5] and Sarah McFarlane[3–5]

[1]Graduate Program in Neuroscience, University of Calgary, Calgary, Canada
[2]Department of Biochemistry and Molecular Biology, University of Calgary, Calgary, Canada
[3]Department of Cell Biology and Anatomy, University of Calgary, Calgary, Canada
[4]Hotchkiss Brain Institute, University of Calgary, Calgary, Canada
[5]Alberta Children's Hospital Research Institute, University of Calgary, Calgary, Canada

PURPOSE. Pathological blood vessel growth in the eye is implicated in several diseases that result in vision loss, including age-related macular degeneration and diabetic retinopathy. The limits of current disease therapies have created the need to identify and characterize new antiangiogenic drugs. Here, we identify the secreted chemorepellent semaphorin-3fa (Sema3fa) as an endogenous anti-angiogenic in the eye.

METHODS. We generated a CRISPR/Cas9 *sema3fa* zebrafish mutant line, *sema3fa^(ca304/304)*. We assessed the retinal and choroidal vasculature in both larval and adult wild-type and *sema3fa* mutant zebrafish.

RESULTS. We find *sema3fa* mRNA is expressed by the ciliary marginal zone, neural retina, and retinal pigment epithelium of zebrafish larvae as choroidal vascularization emerges and the hyaloid/retinal vasculature is remodeled. The hyaloid vessels of *sema3fa* mutants develop appropriately but fail to remodel during the larval period, with adult mutants exhibiting a denser network of capillaries in the retinal periphery than seen in wild-type. The choroid vasculature is also defective in that it develops precociously, and aberrant, leaky sprouts are present in the normally avascular outer retina of both *sema3fa^(ca304/304)* larvae and adult fish.

CONCLUSIONS. Sema3fa is a key endogenous signal for maintaining an avascular retina and preventing pathologic vascularization. Furthermore, we provide a new experimentally accessible model for studying choroid neovascularization (CNV) resulting from primary changes in the retinal environment that lead to downstream vessel infiltration.

Keywords: angiogenesis, semaphorin, zebrafish, retinal pigment epithelium, vasculature

The retina is a highly metabolic structure, with the greatest energy demand coming from photoreceptors and the retinal pigment epithelium (RPE).[1] Vascularization of the eye during development attempts to match neural activity with metabolic support, providing the appropriate number and distribution of vessels to supply nutrients and oxygen. Yet, the outer retina is avascular, with nutrients and oxygen diffusing across the RPE from a dense plexus of extraocular vessels. The positive and negative signaling that regulates the formation of the eye vasculature, while maintaining the avascularity of the outer retina, however, is incompletely understood.

The embryonic retina becomes perfused by two vessel beds.[2] The hyaloid, or retinal, vasculature consists of an intraretinal plexus that nourishes the inner portion of the retina, whereas the choroid plexus supports the RPE and photoreceptors of the outer retina. In retinal diseases such as retinopathy of prematurity, diabetic retinopathy, and the wet form of age-related macular degeneration (AMD), blood vessels grow aberrantly within the retina, which can result in serious vision loss.[3] Thus we need to determine the molecular barriers that normally prevent vessel growth in the retina.

The vessels that grow aberrantly within the neural retina in vascular retinal diseases are often weak and leaky and give rise to pathology. This is true of choroidal retinopathies such as the wet form of AMD,[4] where there is pathological angiogenesis of the outer retina from the surrounding choroid. In this process, termed choroid neovascularization (CNV),[5,6] vessels enter the subretinal space as a result of both increased expression of the key angiogenic molecule, vascular endothelial growth factor (VEGF), and tears to the extracellular matrix rich Bruch's membrane. The infiltrating vessels can leak, which results in macular edemas and detachment of either the RPE or retina. Anti-VEGF therapy is the only current treatment available for wet AMD but is somewhat limited in its effectiveness.[7] Aberrant growth of normally quiescent vessels also underlies the pathology of the inner retina that manifests in proliferative diabetic retinopathy, venous occlusion, and retinopathy of prematurity.[4] Here, regions of ischemic retina trigger

neovascularization, a process that, similar to the choroidal retinopathies, is VEGF or hypoxia driven.

The molecular mechanisms that normally limit vessel outgrowth in the embryonic and adult eye are poorly understood. Impairment of signaling by secreted semaphorin 3s (SEMA3s) may alter vessel growth during retinal disease.[8–10] For instance, reduced transcript levels for the chemorepellent SEMA3F are found in RPE isolates from patients with wet AMD,[8] and exogenous SEMA3F is a powerful antiangiogenic in in vitro and in vivo mouse CNV models.[8,11] These studies raise the interesting possibility of an endogenous role for SEMA3F as an antiangiogenic secreted by eye cells that prevents choroidal vessels from invading the outer retina.

In zebrafish, the retina is nourished by choroid and hyaloid vessels, but intraretinal plexuses do not form as they do in mice and primates.[12–14] The avascularity of the zebrafish neural retina makes it an excellent model for the study of molecular regulators of vascular retinopathies. Here, we generate a *sema3fa* zebrafish mutant by CRISPR/Cas9 gene editing[15] to show that Sema3fa, expressed both by the RPE and the neural retina, regulates the growth of blood vessels that support the inner and outer regions of the larval and adult eye. In larvae, loss of Sema3fa causes an overgrowth of the intraocular hyaloid vasculature and aberrant retinal infiltration of leaky blood vessels from the choroid. These phenotypes persist in the adult, arguing for an ongoing role for Sema3fa in limiting vessel growth. Of note, we have developed the first model of vascular retinopathy that arises from retina-associated changes in the signaling environment of the blood vessels, and not from genetic manipulations of the blood vessels or artificially induced vascularization.

METHODS

Zebrafish Husbandry

Zebrafish (*Danio rerio*) were maintained according to standard procedure on a 14-hour light/10-hour dark cycle at 28°C. Embryos were obtained by natural spawning, raised in E3 medium supplemented with 0.25 mg/L methylene blue, and staged by convention.[16,17] In some experiments, pigmentation was inhibited by adding 0.003% (w/v) 1-phenyl-2-thiourea to E3 medium supplemented with 0.25 mg/L methylene blue at 24 hours post fertilization (hpf). The University of Calgary Animal Care Committee approved all procedures, and we have adhered to the recommendations detailed in the ARVO Animal Statement.

Generation of the *Sema3fa^{ca304/304}* CRISPR Mutant

To generate a genetic knock-out using the CRISPR/Cas9 system a sgRNA targeting *sema3fa* exon 1 (GAAGACTCGTGGAACAGAGG**)** was selected following CHOPCHOP query (Montague et al., 2014)[18] and analysis of secondary structure using Vienna RNAfold Prediction (rna.tbi.univie.ac.at). The sgRNA was transcribed using the SP6 Maxi Kit (Ambion) and *cas9* mRNA was transcribed from a plasmid (Addgene plasmid no. 47322) using mMessage Machine T7 (Thermo Fischer Scientific, Waltham, MA, USA). One-cell stage Tupfel Long (TL) fin embryos were injected with a 1 nL mix of approximately 56 to 60 pg sgRNA and 190 pg *cas9*

TABLE. SgRNA and PCR Primers

Sema3fa sgRNA (5'-3' Sequence)	GCATTTAGGTGACACTATAGA-GAAGACTCGTGGAACAGAGGg-ttttagagctagaaatagcaag
qPCR Primers	
sema3fa forward	GGCACAGGGTTTTCTGCAAG
sema3fa reverse	CCAGGCTCCAGTCGGAAAAT
vegfaa forward	GTGCAGGATGCTGTAATGATGAGG
vegfaa reverse	AATTATGCTGCGATACGCGTTG
vegfab forward	TGCTGAACACAGTGAATGCCAG
vegfab reverse	TCCAAAGGGACGGTTGTAGAGTG

mRNA. RNA was quantified by using a Nanodrop spectrophotometer (Thermo Fisher Scientific). Mosaic embryos were raised to adulthood and crossed with TL fish to identify founders. Genotyping was performed on either single 24 hpf embryos or caudal fin clippings from tricaine methanesulfonate (MS222; 160mg/L) anesthetized adult fish. Genomic DNA was extracted as described previously,[19] and amplified by PCR using primers around the expected mutational site (S3fa F:5′-CCCATGCAGGACTGATAAATCT, S3fa R:5′-AGGAAAGCAGTGGTTGTCATCT). Amplicons were sequenced at the University of Calgary DNA Core facility for definitive genotype confirmation. Heterozygous F1 adult fish (Δ2 bp) were outcrossed to TL fish, and F2 heterozygous progeny were intercrossed to generate genotypes (wild-type [WT], heterozygous, homozygous mutant). The *sema3fa^{ca304/304}* fish were maintained as heterozygotes for all initial experiments and thereafter maintained as homozygotes and WT siblings for future embryonic collection. Ongoing familial generations were derived from heterozygous incrosses. *Tg(- 6.5kdrl:mCherry)^{ci5}* was used as an outcross for the *sema3fa* mutant to label endothelial cells.[20]

Real Time Quantitative PCR (RT-qPCR)

Total RNA from 3-5 embryos at specific developmental ages was prepared using the TRIzol reagent (Invitrogen) extraction method.[21] First strand cDNA was made using the Superscript II RT-PCR (Invitrogen, 11904-018) protocol. Each RT-qPCR had a 10 μl final volume containing 0.5 μl of cDNA, 500 nM of each primer and 5 μl of Quantifast SYBR Green PCR Kit (Qiagen). RT-qPCR primers are listed in the Table. An Applied Biosystems QuantStudio 6 Real-Time PCR system (Thermo Fisher Scientific) was used for all experimental procedures. Gene expression was normalized relative to reference gene *β*-actin. Reactions were performed in three technical replicates, and all results made from three independent biological replicates. Fluorescence was measured after each cycle and a melt curve analysis conducted to verify the purity of samples. Equipment software automatically calculated baseline, threshold Cq, and fold changes.

In Situ Hybridization

WT Tupfel Long Fin (TL) fish were used for in situ hybridization (ISH). Digoxigenin RNA probes were synthesized as described previously.[22] The *vegfaa* probe was made as described previously.[23] Additional probes were generated from PCR products containing an SP6 or T7 RNA polymerase binding sequence on the reverse primer. Probes used included the follow-

ing: *sema3fa* - F CGTGTCCGGGTCTGTGTTTA, R +T7 GAAATTAATACGACTCACTATAGGGCCAAAAAGGCT-GTGCTTCCC; *npn2a* F GGGAGAAATCCCTGCG-GAAA, *npn2a* R +SP6 GCATTTAGGTGACAC-TATAGACTCTGATGGGCGGGTATTC; and *npn2b* F TCCGGGATGGGAACTCAGAT, *npn2b* R +S6 GCATT-TAGGTGACACTATAGAATCGGCCGTCATAGAAGCTG.

Whole mount ISH was performed as described previously with some minor modifications.[22] The steps with gradient changes in hybridization buffer, 2 × SSC- and 0.2 × saline sodium citrate (SSC)–phosphate-buffered saline solution (PBS) with 0.1% Triton X-100 (PBST) solutions, were omitted. The 2 × SSC step was carried out at 70°C and 0.2 × SSC at 37°C. The embryo blocking step was omitted; instead embryos were incubated in anti-DIG-AP Fab fragments antibody (Roche, Basel, Switzerland) solution in blocking buffer at room temperature for two hours. Embryos were washed in alkaline buffer, transferred to a 24-well culture dish (Thermo Scientific), and stained by NBT/BCIP (Roche) in a 2.5/3.5 μL/mL ratio, respectively. After staining, embryos were fixed in 4% paraformaldehyde (PFA) and washed in 1 × PBST. To increase permeability samples were incubated in 5 μg/mL proteinase K for 30 minutes before addition of the riboprobe. Whole mount ISH samples were embedded in JB4 medium (Polysciences, Warington, PA, USA) as described in Sullivan-Brown et al.[23] and sectioned at 7 μm using a Leica microtome (Leica, Wetzlar, Germany). ISH of adult eyes on transverse 12 μm bleached cryostat sections on glass slides was performed similarly, and slides coverslipped using Aquapolymount (Polysciences Inc, Warrington, PA, USA).

Histology

Embryos were fixed in 4% PFA overnight at 4°C, washed in PBST, and placed in 35% sucrose (EM Science; Thomas Scientific, Swedesboro, NJ, USA) in PBS overnight at 4°C. Embryos were embedded in molds containing optimal cutting temperature (Tissue-Tek; Sakura Finetek USA, Inc., Torrance, CA, USA), and frozen sections were made on a Leica CM 3050S cryostat at 12 μm or 40 μm (Leica). For immunohistochemistry, samples were blocked in 10% bovine serum albumin, 2% normal sheep serum in PBST for 30 minutes and transferred to primary antibody solutions in 1/10 blocking buffer overnight at 4°C. Samples were then washed with PBST and incubated in secondary antibody (Alexa Fluor 488/555 rabbit/mouse; Abcam, Cambridge, MA, USA) supplemented with 5 mg/mL Hoechst (Sanofi-Aventis, Paris, France) in PBST for 45 minutes. Embryos were fixed and imaged or processed further for sectioning. Primary antibodies used were Zpr2 (1:1000, ZIRC), ZO-1 (1:100, Molecular Probes) and glutamine synthetase (Clone GS-6 from Millipore, Lot 2795087, 1:500; Millipore, Burlington, MA, USA). To detect apoptotic cells in situ, the ApopTag Peroxidase In Situ Apoptosis Detection kit (Millipore) was used as per the user guide; however, the diaminobenzidine staining was carried out overnight.

Hematoxylin and Eosin Staining

Hematoxylin and eosin staining of plastic sections was carried out in accordance with the protocol described previously,[24] with the following modifications. Acid and base washes were omitted, Harris modified hematoxylin solution (Sigma-Aldrich Corp., St. Louis, MO, USA) and eosin

Y were used, and regular tap water was used instead of the prescribed substitute. Slides were air-dried for 15 minutes and coverslipped using Permount (Fischer Scientific).

Retinal Flat Mounts

Adult retinal flat mounts were prepared as described previously.[25] Briefly, adult *kdrl* transgenic WT and homozygous mutants were anesthetized in Tricaine (Sigma-Aldrich Corp.), cervically dislocated and fixed in 4% PFA. Eyes were submerged in PBS and enucleated, the anterior segment removed, and short cuts made to relax the optic cup into a flat preparation. Retinas were placed on slides and coverslipped using AquaPolymount. Primary vessel length and diameter were measured as described previously.[26] Primary vessel length and width measurements were made on the primary vessel between the optic nerve head base and first vessel bifurcation. Intercapillary distance measurements were made near the periphery of the retinal flat mounts, an area where retinal arterial capillaries anastomose with circumferential vein capillaries.[27] Measurements were averaged across all quadrants.

Confocal Microscopy

For confocal microscopy, live embryos were imaged on the Zeiss LSM 700 microscope after mounting in 0.8% to 1% low melting point agarose (Invitrogen, Carlsbad, CA, USA) on a glass-bottom dish. Slices were taken at intervals from 1 to 5 μm on a 10× or 20× objective and subjected to two times averaging. Similar parameters were used for slides and retinal flat mounts (1 μm slices). Maximal projections were made and the vessel of the optic nerve head was determined. Z-stacks were processed in Zen Blue as maximal projections and compiled using Inkscape 0.92.3.

Statistical Analysis

All statistical analysis was performed using Prism 7 software (GraphPad, San Diego, CA, USA). Unpaired, nonparametric tests were used in all statistical tests. For situations containing two experimental conditions a Mann-Whitney U test was used. When groups of three or more experimental conditions were compared, a nonparametric one-way ANOVA with a Kruskal-Wallis test was used. All data sets for quantification (qualitative scorings or absolute measurements) were analyzed in a blinded fashion.

Western Blot Analysis

A custom polyclonal antibody made against zebrafish Sema3Fa peptide CIGDDPMAHKKKDLK was generated in rabbits by GenScript USA Inc (Piscataway, NJ, USA). For Western blot, 5 to 6 days post-fertilization (dpf) WT and mutant embryos were collected. The protein was lysed in RIPA buffer (20 mM Tris-HCl [pH 7.5] 150 mM NaCl, 1 mM Na2 EDTA 1 mM EGTA 1% NP-40 1% sodium deoxycholate 2.5 mM sodium pyrophosphate 1 mM), separated on a 10% polyacrylamide gel (approximately 60 ug/lane), and transferred to a polyvinylidene difluoride membrane (Bio-Rad) by using standard procedures. Membranes were immunoblotted with the zebrafish *sema3fa* antibody (1/1000 dilution) or goat anti-ß-actin (C-11, 1/1000 dilution; Santa Cruz Biotechnology Inc.), followed by a specific peroxidase-conjugated secondary antibody (1/2000 dilution; Jack-

son Immunoresearch). Sema3fa antibody specificity was determined by preincubation of the immunoserum (one hour at room temperature) with an excess of the Sema3fa peptide epitope.

RESULTS

Sema3fa is Expressed by the RPE in Development and Adulthood

SEMA3F is expressed by the RPE of the outer mouse retina.[8] As such, we asked by whole mount in situ hybridization if *sema3fa* mRNA was expressed by the zebrafish RPE from the embryo into the adult. The newly formed RPE at 24 hpf did not express *sema3fa*, but *sema3fa* mRNA was present in the RPE at 72 hpf as the retinal layers form (Fig. 1B). These data agree with previous gene expression analysis of isolated 52 hpf zebrafish RPE, which point to *sema3fa* as the only Sema expressed by the RPE at this stage.[28] The *sema3fa* expression was maintained in the RPE through the 7 dpf) larval stage (Figs. 1A, 1B) and into the adult (Fig. 1D). The similar expression of SEMA3F in the SSC mouse, human and zebrafish RPE are supportive of a conserved role. Of note, *sema3fa* mRNA was expressed robustly in the proliferative ciliary marginal zone (CMZ) and inner nuclear layer, containing retinal interneurons, from larval stages and into the adult (Figs. 1A, 1B, 1D). To understand which cells might respond to *sema3fa*, we investigated mRNA expression of *nrp2a* and *nrp2b*, the zebrafish orthologues of the main Sema3f receptor, Nrp2.[29–31] Although *nrp2a* shows weak expression in the inner retina (Fig. 1E), *nrp2b* appears to be expressed by endothelial cells of the hyaloid vessel running proximate to the optic nerve head (Fig. 1F; yellow arrow) and the choroid vessels that cover the back of the eye (Figs. 1F, 1G; black arrows).

To investigate an endogenous role for Sema3fa in regulating eye vessel beds, we used CRISPR/Cas9 gene-editing technology to generate a *sema3fa* mutant, by using a sgRNA to target exon 1 (Fig. 1H). A founder was identified with a two–base pair deletion, which was predicted to generate a 76–amino acid protein, because of a premature truncation within the 500–amino acid SEMA domain necessary for intracellular signaling[32] (Fig. 1I). RT-qPCR indicated a reduction in *sema3fa* mRNA levels in mutant embryos as compared to WT at 48 hpf (Fig. 1J), suggestive of nonsense-mediated mRNA decay. Furthermore, Western blot analysis revealed that Sema3f protein was absent in *sema3fa^{ca304}* mutants, indicating that the mutants are null for *sema3fa* (Fig. 1K). No differences were found in either head-to-tail body length (Fig. 1L,M), or the ratio of the lateral eye to body size (Fig. 1N) in embryos of the different genotypes from 36–72 hpf. These data suggest no gross abnormalities in the development of *sema3fa* mutant embryos or their eyes.

Sema3fa Refines and Limits Retinal Vessel Branching in the Larvae and Adult

To directly investigate eye vessel growth in an environment that lacked Sema3fa, *sema3fa* mutants were outcrossed to *Tg(kdrl:mCherry)^{ci5}*, in which all endothelial cells are labeled by mCherry.[20] Resulting heterozygote adults were incrossed to generate WT and homozygous mutant lines. All subsequent analyses were performed on a mix of embryos generated from either heterozygous incross matings or the established monogenic transgenic lines.

The hyaloid vessel enters the eye and branches to form a network of vessels covering the medial aspect of the lens.[4,12,33,34] In zebrafish, the hyaloid detaches from the lens beginning at 15 dpf, adheres to the inner limiting membrane, and forms the adult retinal vasculature.[12] In mouse, the hyaloid vessel regresses completely and regrows to form the retinal vasculature.[4] Entry of the hyaloid vessel into the retina was unaffected in the *sema3fa* mutants as assessed by confocal live-imaging at 24 hpf (Figs. 2A, 2B).[33] Additionally, at 72 hpf the branched hyaloid network around the lens formed normally in mutant and WT embryos (arrows, Figs. 2C, 2D). The nasal ciliary artery that forms part of the superficial ocular vasculature[35] was also evident in all WT and mutant 72 hpf embryos and 7 dpf larvae (72 hpf, WT $n = 4$ embryos, *sema3fa^{ca304}* $n = 4$; 7 dpf, WT $n = 11$, *sema3fa^{ca304}* $n = 9$) (Figs. 2C, 2D). Thus Sema3fa appears to have no role in the establishment of the vasculature of the early retina.

Between 4 to 5 dpf, remodeling reduces the complexity of the zebrafish retinal vessels by a refinement process where extraneous connections are retracted. Given the postembryonic expression of *sema3fa* in the CMZ and neural retina, close to the hyaloid vessel bed, we asked whether vessel refinement was affected by the loss of Sema3fa. Although the hyaloid network was refined to a simplified stereotypic pattern in 91% of WT embryos (Figs. 2E, 2E'), all heterozygous and homozygous *sema3fa* mutants (Figs. 2F, 2G) retained complex hyaloid vessel networks, with interconnections throughout the plexus. These data suggest that Sema3fa is necessary for the refinement of the embryonic hyaloid vasculature.

To determine whether patterning of the hyaloid network continued to be impacted by the absence of Sema3fa, we assessed the retinal vasculature of adult animals. The hyaloid network comes to adhere to the inner limiting membrane of the retina,[12] so the complexity of the vessel network was visualized readily in retinal flat mounts of transgenic *sema3fa+/+* and *sema3fa−/−* 5-month-old adult *Tg(kdrl:mCherry)* fish (Figs. 3A, 3B). We measured three parameters of vessel growth; primary vessel length (Fig. 3C), as measured from the optic nerve head to the first branching event, primary vessel width (Fig. 3D), and capillary spacing in the retinal periphery (Fig. 3E).[26] Primary vessel length was significantly shorter (Fig. 3C), and the width of these vessels significantly thinner (Fig. 3D), in mutants as compared to WT. Finally, capillaries in the retinal periphery (Figs. 3A', 3B'), where arterial capillaries anastomose with circumferential vein capillaries,[27] were closer to one another in the mutants (Fig. 3E). Furthermore, more intercapillary connections and sprouts (Figs. 3A', 3B'; arrows) were apparent in the mutants as compared to the WT retinas (Fig. 3F). Thus Sema3fa is necessary for both establishing and maintaining a properly ramified vascular tree structure in the retina throughout life.

The Choroid Plexus Undergoes Neovascularization in *sema3fa* Mutant Retina

In zebrafish, the choroid plexus at the back of the eye is first observed by 5.75 dpf.[36] At this time point, and through to the adult, *sema3fa* is expressed by the adjacent neural retina and RPE (Fig. 1). Thus we live-imaged the choroidal vessel network of 6 dpf *Tg(kdrl:mCherry)* embryos to assess the impact of Sema3fa loss. We found that *sema3fa−/−* embryos exhibited a choroid plexus ($N = 1$, $n = 3/3$)
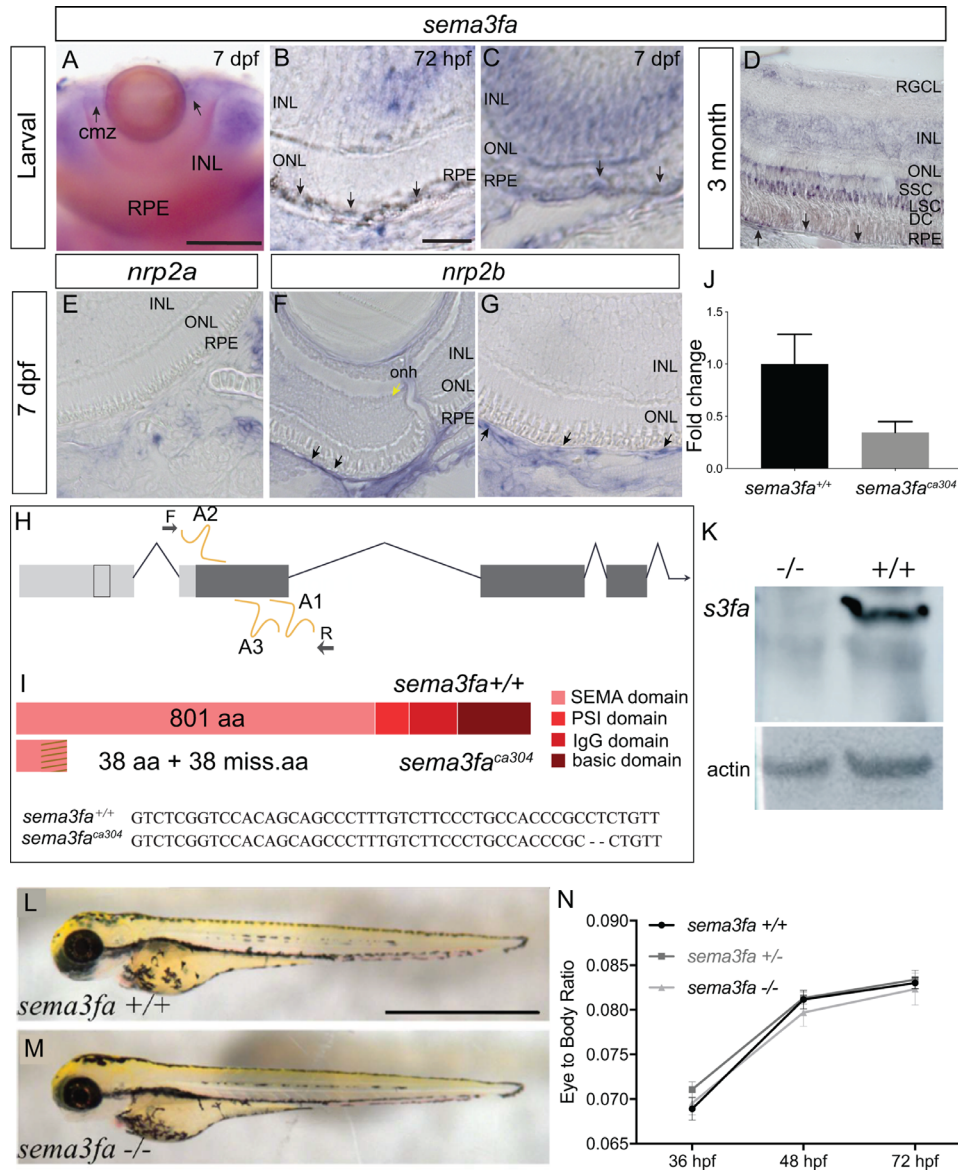
FIGURE 1. *Sema3fa* is expressed by the RPE and inner retina of larval and adult zebrafish. **(A–D)** *sema3fa* RNA ISH in whole mount **(A)** and retinal sections **(B–D)**. ISH signal is detected in the retinal pigment epithelium (RPE) during development **(A–C)** and into adulthood **(D)**. In larval and adult retina, *sema3fa* is also expressed strongly in the inner nuclear layer (INL) and CMZ, with expression in the outer nuclear layer (ONL) observed in the adult. **(E–G)** Expression at 7 dpf of mRNA for the known Sema3fa receptor *nrp2b* **(F,G)** but not *nrp2a* **(E)** by the endothelial cells of the retinal artery that runs alongside the optic nerve head (yellow arrow) and the choroid vessels lining the back of the eye (*black arrows*). Note that to minimize the pigment of the RPE, retinal sections were either from larvae treated at 24 hpf with 1-phenyl-2-thiourea **(A–C, E–G)**, or were bleached **(D)**. **(H)** Chromosomal overview of the *sema3fa* locus targeted by CRISPR/Cas9 mutagenesis to exon 1 (guide RNA: A1-3) and primers used to identify the mutation. UTR: untranslated region; F: forward primer; R: reverse primer. **(I)** Schematic representation of WT and premature stop codon mutant proteins. *sema3fa^{ca304}* fish have a 2 bp deletion (dashes) and produce a predicted product of 76 aa. Dashes represent missense amino acids (miss.aa). **(J)** RT-qPCR of *sema3fa* mRNA levels in WT and *sema3fb^{ca304}* embryos at 48 hpf suggest nonsense mediated decay of mRNA transcript ($N = 3$). Error bar represents standard error of the mean (SEM). **(K)** Western blot of protein isolated from 5-6 dpf WT and *sema3fa^{ca304}* mutant fish processed with a custom-made antibody against zebrafish Sema3fa. The antibody recognizes a protein of the appropriate size for Sema3fa in WT fish, which is absent in the mutants. Loading control is ß-actin. **(L, M)** Lateral views of 72 hpf WT **(H)** and *sema3fa^{ca304}* **(I)** fish. **(N)** The ratio of eye width to anterior-posterior body length, measured along the antero-posterior axis, at 36, 48, and 72 hpf, arguing that there are no gross abnormalities in body or eye growth in the *sema3fa* heterozygote ($n = 10$) and homozygote ($n = 4$) mutant embryos as compared to WT ($n = 10$). *Scale bars*: **A**: 100 µm; **B**: 15 µm; **L**: 1 mm.

before WT embryos ($N = 1$, $n = 0/3$). Because the presence of the choroid plexus was somewhat variable at 6 dpf in WT, we used 7 dpf for quantitation, when most WT larvae exhibit a choroid plexus. Although a nascent choroid plexus was present in 88% of WT embryos (Fig. 4A), the plexuses were overgrown or advanced in 69% of heterozygous (Fig. 4B) and 71% of homozygous (Fig. 4C) *sema3fa* embryos. These data suggest that precocious choroid plexus growth occurs when Sema3fa signals are removed from the retina.
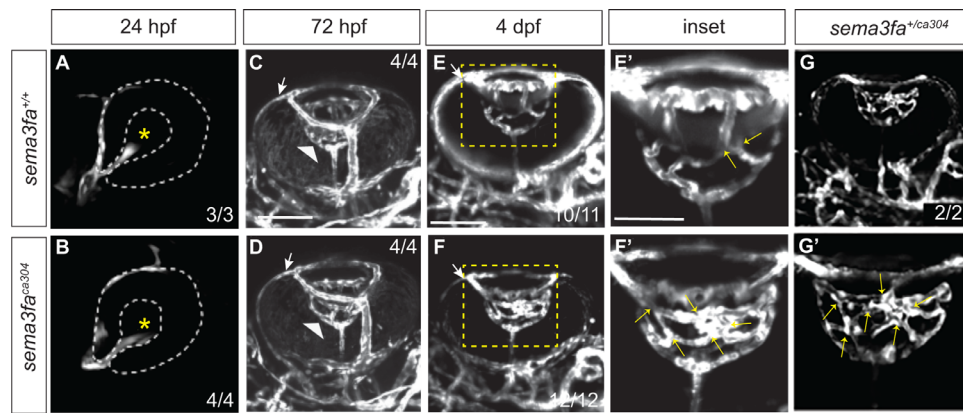
FIGURE 2. Sema3fa is required to refine and limit retinal vessel branching in the larval eye. Live imaging of vessels (*white*) in *Tg(kdrl:mCherry)* WT (**A,C,E,E'**) and *sema3fa^ca304^* heterozygous (**G,G'**), and homozygous (**B,D,F,F'**) eyes during retinal intraocular vascular development acquired by confocal microscopy. (**A, B**) In lateral views of WT (**A**) and *sema3fa^ca304^* homozygous embryos, the hyaloid artery (endothelial cells labeled by mCherry) contacts the lens (asterisk) of the retina by 24 hpf ($N = 1$ WT $n = 3$; *sema3fa^ca304^* $n = 4$). (**C, D**) Ventral views of WT (**C**: $N = 1$, $n = 4$) and *sema3fa^ca304^* (**D**: $N = 1$, $n = 4$) eyes reveal that the hyaloid artery (arrowhead) forms a vascular plexus network around the lens by 72 hpf. Also evident is the nasal ciliary artery (*arrows*). (**E–G**) The WT intraocular hyaloid vessel (**E'** is a magnified view of the boxed area in **E**) undergoes remodeling between 4-5 dpf to simplify the network (Hartsock et al., 2014). At 4 dpf, the numbers of vessel crossovers (arrows) are increased in *sema3fa* heterozygous (**G,G'**: $N = 1$, $n = 2/2$) and homozygous (**F,F'**: $N = 4$, $n = 12/12$) mutant embryos as compared to WT siblings (**E, E'**: $N = 4$, $n = 10/11$ show refinement). *Scale bar*: 100 μm; 50 μm for **E'–G'**.
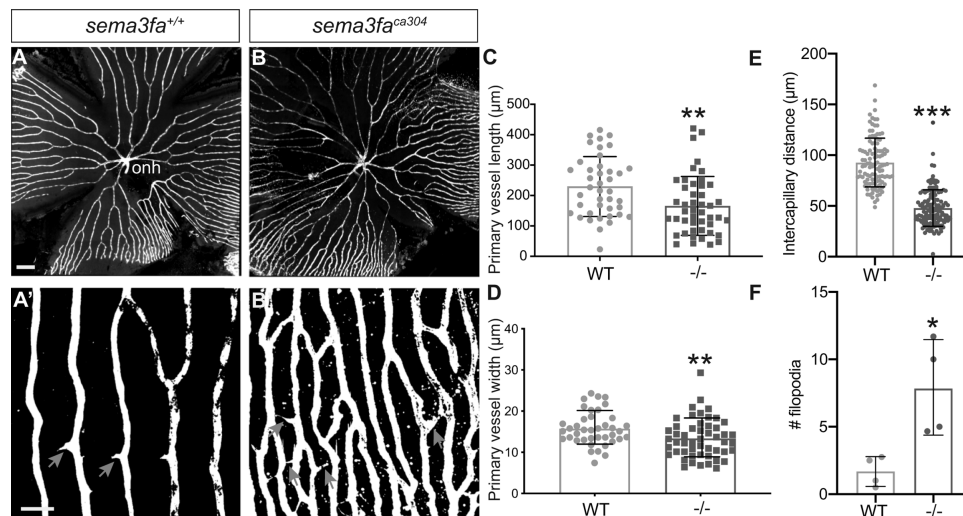

FIGURE 3. Increased vascularization of the retina is observed into adulthood. (**A, B**) Vessels (white) in retinal flat mounts of *Tg(kdrl:mCherry)* WT siblings (**A**) and *sema3fa^ca304^* (**B**) 5 month fish. Capillaries furthest from the optic nerve head (onh) in the peripheral retina are shown in **A',B'**. A greater number of filopodial interconnections between capillaries are present in mutant retina (*gray arrows*). (**C**) Primary vessel length as measured from the optic nerve head (onh) to the first branching event is significantly shorter in mutants (**$P = 0.0016$, $N = 2$, $n = 6$ retinas) as compared to WT siblings ($N = 2$, $n = 6$ retinas). (**D**) The average width of the primary vessels is reduced significantly in mutants (**$P = 0.0078$; $N = 2$, $n = 6$ retinas) as compared to WT ($N = 2$, $n = 6$ retinas). (**E**) Measurement of the intercapillary distance shows that mutant capillaries are more closely spaced ($n = 4$ retinas, $P < 0.0001$) than in WT ($n = 4$ retinas). (**F**) Average number of filopodia in a region of interest in the retinal periphery (WT $n = 4$; *sema3fa^ca304^* $n = 4$; $P = 0.029$). *Error bars* represent standard deviation (SD). Statistics represent the nonparametric Mann-Whitney U test. *Scale bar*: 200 μm (**A**) and 50 μm (**A'**).

Sema3fa −/− Orbital Vasculature is Leaky

We next asked whether the overgrowth of the choroid plexus seen in mutants compromised the physiological avascularity of the retina. To label the retinal and choroid vasculature, we performed fluorescent angiography by using a 2,000,000 MW rhodamine-dextran, a molecule normally too large to pass through vessel walls.[36] We injected the hearts of 8 and 10 dpf WT and mutant embryos with the rhodamine-dextran, fixed the embryos 24 hours after injection, and imaged cryostat-sectioned retinas (Figs. 4D–4O). Vessels were detected within the outer nuclear layer in all of the 8 dpf and 10 dpf (arrowheads Figs. 4I, 4O) mutant larvae, but none of the WT larvae (Figs. 4D–4F, 4L). Of note, dextran accumulated within the neural retina in all of the 8 dpf and most of the 10 dpf (Figs. 4H, 4I, 4N, 4O) mutant larvae, but was largely absent from the WT retinas (Figs. 4E–4F, 4K, 4L). Taken together, these data indicate that in
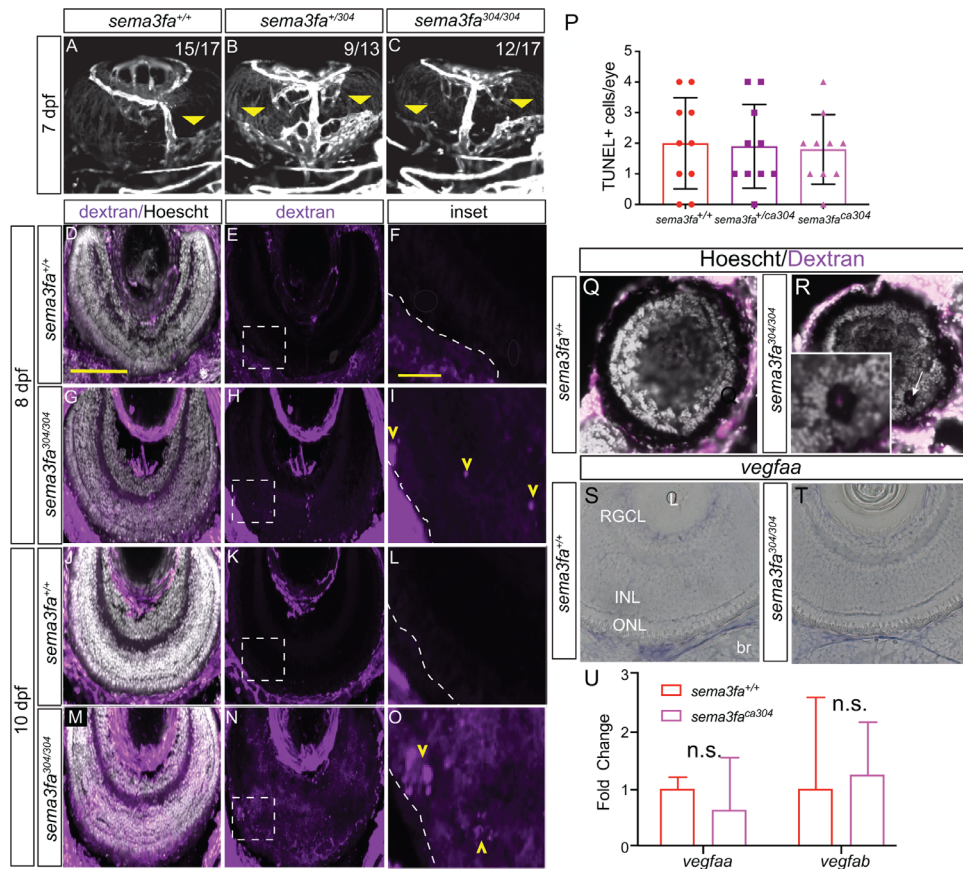
FIGURE 4. The *sema3fa*-deficient embryos present with leaky vessels within the outer retina. **(A–C)** Vessels (white) in ventral views of the eyes of live imaged *Tg(kdrl:mCherry)* 7 dpf larvae. In WT (**A**: $N = 6$, $n = 15/17$) larvae the extraocular choroid plexus (yellow arrowhead) has begun to branch over the back of the retina. Heterozygous (**B**: $N = 4$, $n = 9/13$) and homozygous (**C**: $N = 6$, $n = 12/17$) *semafa^ca304* eyes exhibit a dramatic increase in the choroid vasculature as compared to WT. **(D–O)** Sema3fa deficiency permits the entry of leaky vessels into the neural retina. Thick (40 µm) cryosections through the eyes of embryos injected at 8 dpf (**E–I**) or 10 dpf (**J–O**) with 2,000,000 MW rhodamine dextran and fixed 24 hours later. Sections are counterstained with nuclear label (Hoechst). Blood vessels (*yellow arrowheads*) infiltrate aberrantly into the outer retina of homozygous embryos at 8 dpf (**I**: $N = 2$, $n = 4/4$) and 10 dpf (**O**: $N = 3$, $n = 10/10$), but are not present in WT embryos (**F**: $N = 2$, $n = 4/4$ for 8 dpf; **L**: $N = 2$, $n = 10/10$ for 10 dpf). Dextran is present in the neural retina at 8 and 10 dpf in homozygous mutant eyes (**H, I**: 8 dpf, $N = 2$, $n = 4/4$; **N, O**: 10 dpf, $N = 3$, $n = 8/10$), but is essentially absent from WT (**E, F**: 8 dpf, $N = 2$, $n = 4/4$; **K, L**: 10 dpf, $N = 3$, $n = 9/10$) eyes. *Dashed line* represents the boundary between the RPE and neural retina. *Boxed areas* in **E, H, K,** and **N** are shown magnified in **F, I, L,** and **O**. **(P)** Average numbers of TUNEL+ apoptotic cells in whole mount WT, heterozygous, and homozygote eyes at 7 dpf ($P > 0.99$; $N = 2$, $n = 10$ for each genotype). **(Q, R)** An example of the peripheral retina of a WT (**Q**) and *semafa^ca304* (**R**) 10 dpf larvae, where penetrating pathologic vessels in the mutant appear to disrupt retinal cellular architecture (*arrow*). **(S,T)** *vegfaa* expression in plastic sections of WT (**S**) and *sema3fa* mutant (**T**) 7 dpf retinas. **(U)** RT-qPCR for *vegfaa* and *vegfab* performed on mRNA isolated from WT ($n = 5$) and *semafa^ca304* ($n = 5$) 7 dpf eyes. br, brain; INL, inner nuclear layer; L, lens; ONL, outer nuclear layer; RGCL, retinal ganglion cell layer. *Error bars* are *SD*. *Scale bar*: **D**: 100 µm; **F, I, L, O**: 20 µm.

the absence of Sema3fa, blood vessels invade the normally avascular outer retina and that these invasive vessels are not stabilized properly. Although there was no increase in TUNEL-positive dying cells in the retinas lacking Sema3fa (Fig. 4P), we did find instances where the retinal cellular architecture appeared disrupted by penetrating vessels (Figs. 4Q, 4R).

To address whether the entry of leaky vessels into the eye was solely a larval phenotype, we analyzed in retinal sections the extent of vessel infiltration into WT and mutant adult (five months) *Tg(kdrl:mCherry)* outer retinas (Fig. 5). The mCherry-positive cells were present in most of the mutants (Figs. 5D–5F) and none of the WT siblings (Figs. 5A–5C). To determine whether the vessels remained leaky in the adult, we injected the fluorescent angiography dye into aged (12 month) adult WT and mutant fish. Dextran was present within the neural retina (Fig. 5H) in the majority

of homozygous mutants and none of the WT fish (Fig. 5G), indicating that mutant adult ectopic vessels remain leaky.

Sema3fa Functions as an Endogenous Anti-Angiogenic That Prevents CNV

Increased VEGF expression is thought to drive CNV development in AMD.[5,6] In zebrafish, Vegfa is a potent endothelial cell mitogen necessary for vascular development and drives retinal and choroidal vascularization.[37,38] As such, we asked whether the *sema3fa* mutant CNV phenotype was due to an upregulation of *vegfa* expression in the outer retina. Zebrafish have a duplicated *vegfa*, with *vegfaa* and *vegfab* isoforms.[39] Of note, previous reports indicate that after the main period of embryonic angiogenesis there are only low or undetectable levels of *vegfaa* and *vegfab*, respec-
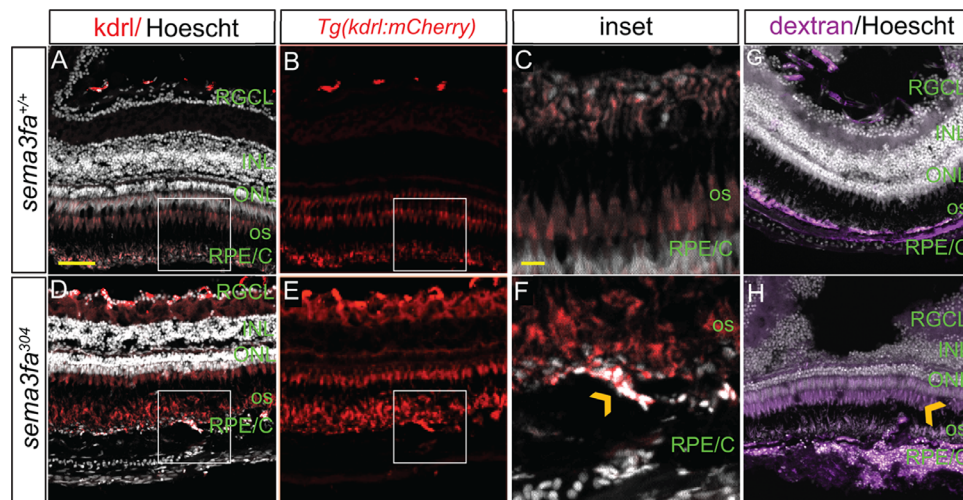
FIGURE 5. Vessel infiltration persists in the adult *sema3fa* mutant retina. (**A–H**) Cryosections made through the retinas of *Tg(kdrl:mCherry) sema3fa* WT (**A–C**) and mutant (**D–F**) 5 month old siblings. Nuclei are labeled by Hoechst (white). Blood vessels were detected in the area of the photoreceptor outer segments (os) in the majority of *semafa*^{ca304} eyes ($N = 1$, $n = 3/4$), but not in WT retinas ($N = 1$, $n = 4$). **C** and **F** are magnified views of the boxed regions in **B** and **E**. Yellow chevron points to blood vessel. (**G, H**) One-year-old adult *sema3fa*+/+ (**G**) and *sema3fa*−/− (**H**) fish were injected with 2,000,000 MW rhodamine dextran (*purple*) and fixed 4 hours later. Thick (40 μm) eye cryosections counterstained with nuclear label (Hoechst) reveal leakage of dye (*purple, yellow chevron*) in the neural retina of *semafa*^{ca304} fish (**H:** $n = 3/5$), but not WT siblings (**G:** $n = 3/3$). inl, inner nuclear layer; onl, outer nuclear layer; RGC, retinal ganglion cell layer; RPE/C, retinal pigment epithelium/choroid. *Scale bar*: 50 μm. *Scale bar of inset*: 10 μm.

tively, in the adult zebrafish retina.[40] In agreement, *vegfaa* (Figs. 4S, 4T) and *vegfab* mRNAs detected by whole mount ISH were present at similarly low levels in the eyes of 7 dpf WT (*vegfaa* $N = 2$, $n = 15$; *vegfab* $N = 1$, $n = 7$) and mutant (*vegfaa* $N = 2$, $n = 9$; *vegfab* $N = 1$, $n = 4$) larvae. That neither isoform was upregulated in *sema3fa*^{ca304} eyes as compared to WT was confirmed by RT-qPCR of cDNA from eyes isolated from 7 dpf fish (Fig. 4U). These data suggest that vessel infiltration into the neural retina is not driven primarily by an increase in *vegfa* expression.

Breaks in the RPE can provide a conduit for blood vessel sprouts from the choroid plexus to enter the neural retina.[41] To analyze whether the RPE was intact in *sema3fa* mutant fish, we first looked at histological sections stained by hematoxylin/eosin at 72 hpf and 8 dpf. The *sema3fa* mutants showed no obvious disruption or thinning of the RPE (Fig. 6A,B), and the epithelium appeared to exhibit the appropriate morphology and polarity, with apical microvilli present in both the WT and *sema3fa*^{ca304} retinas (arrows, Figs. 6A', 6B'). Additionally, the Zpr2 antibody showed immunostaining of the RPE[42] that was indistinguishable between WT and mutant retinas at 7 dpf (Figs. 6C, 6D). The outer limiting membrane (OLM), which consists of junctions between the Müller glia and the inner segment of the photoreceptors, contributes to the outer blood-retinal barrier.[43] Because the OLM is reported to be mature by 5 dpf,[44,45] we investigated the OLM at this time point with ZO-1 that marks adhesion junctions between photoreceptors and Müller glia (Figs. 6E, 6F), and phalloidin, which labels F-actin (Figs. 6G, 6H).[46] Punctate ZO-1 and uninterrupted F-actin labeling of the OLM was observed in both genotypes. F-actin labeling at the OLM still showed no disruption at 15 dpf (Figs. 6K', 6L'), nor did the apical endfeet processes of the Müller glia at the OLM at either 7 dpf (Figs. 6I, 6J) or 15 dpf (Fig. 6K, 6L), as labeled by an antibody against glutamine synthetase or by EGFP in a *Tg(gfap:egfp)* background, respectively. These data support the idea that the OLM is present, with the required Müller

glia endfeet and cell adhesion (ZO-1) features intact, in mutant retinas well past the time that aberrant entry of choroid angiogenic sprouts is evident in the outer retina. These results suggest that the ectopic retinal entry of blood vessels with Sema3fa loss arises from the loss of an endogenous anti-angiogenic signal, rather than an underlying RPE or outer retinal barrier dysfunction.

DISCUSSION

Here we demonstrate that Sema3f restricts the growth of the eye vasculature from embryo to adult. Specifically, endogenous Sema3f maintains the physiologic avascularity of the outer retina and limits the extent of the retinal vascular network. Interestingly, the impact of Sema3fa loss differs for the two vessel beds. Although the intraocular vasculature fails to undergo its normal refinement, the extraocular vasculature grows precociously, and leaky vessels infiltrate into the larval and adult neural retina. This work provides *sema3fa* knockout zebrafish as a novel model to understand the cellular and molecular mechanisms of choroidal retinopathies that arise from an environmental change in the outer retina and to test novel antiangiogenics via high throughput drug screening.

A possible explanation for the choroid vessel phenotype is that Sema3fa is required for normal development of the RPE or outer retinal-blood barrier, to which the OLM contributes. Although we cannot rule out this possibility, our data showing no gross defects in either the RPE or OLM and the persistence of *sema3fa* expression by the inner nuclear layer and RPE into the adult, suggests an ongoing role for this protein. Instead, we propose a model whereby Sema3fa locally represses vascular growth (Figs. 6M, 6N). In the outer retina, we suggest that Sema3fa arising from either the RPE and/or the inner nuclear layer inhibits choroid vessel sprouting (Fig. 6I). In support, *sema3fa* mRNA is expressed by
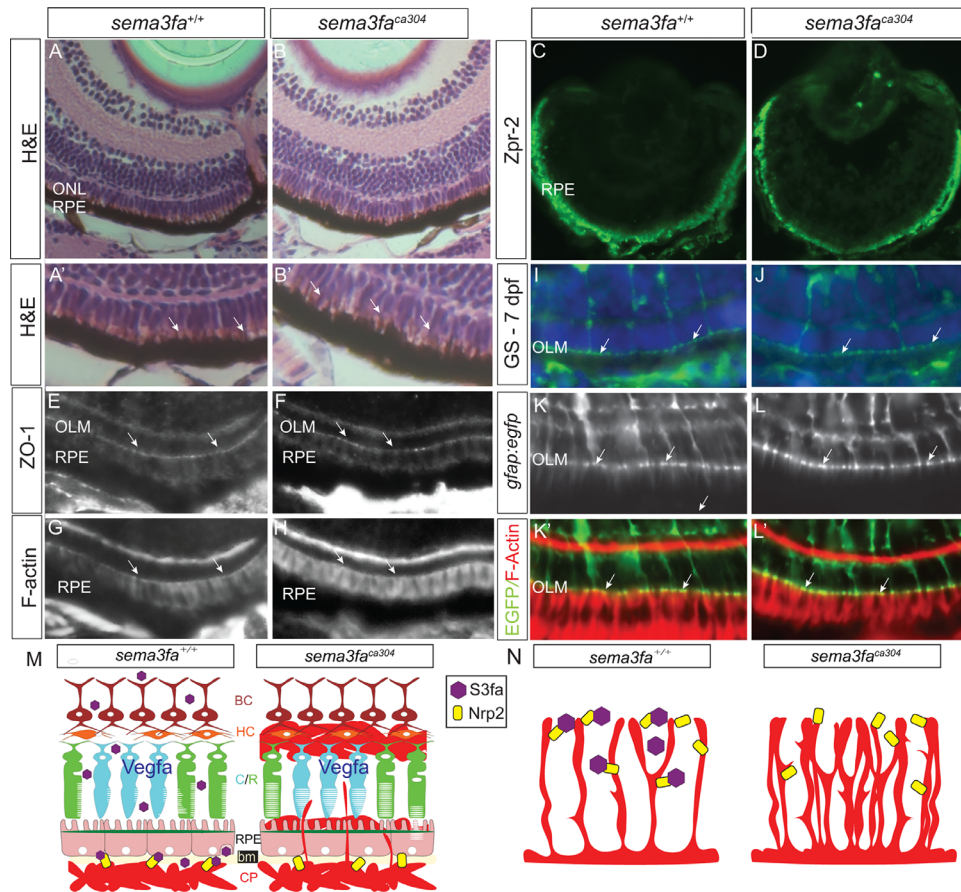
Figure 6. No obvious disruption of the RPE and outer limiting membrane with the loss of Sema3fa. **(A, B)** Transverse sections of 8 dpf WT and *sema3fa^{ca304}* mutant light-adapted retinas labeled with hematoxylin and eosin. A higher power view of the RPE is shown in **A'** and **B'**. No obvious gaps are seen in the RPE, and apical microvilli (*arrows*) are evident in both genotypes ($N = 3$, $n = 9$ at 72 hpf for both genotypes; $N = 2$, $n = 10$ at 8 dpf for both genotypes). **(C, D)** Immunolabeling of the RPE with the Zpr2 antibody is comparable in WT ($N = 2$, $n = 9$) and mutant ($N = 2$, $n = 9$) retinas. **(E–H)** No obvious disruption of the outer limiting membrane (OLM; *arrows*), as stained with an antibody for the adhesive junction protein ZO-1 ($N = 2$, $n = 10/10$ WT eyes; $n = 7/7$ *sema3fa^{ca304}* eyes) and phalloidin that labels F-actin ($N = 3$, $n = 15/15$ WT eyes; $n = 16/16$ *sema3fa^{ca304}* eyes). **(I, J)** Glutamine synthetase immunolabeling of the Müller glia in WT (I; $N = 2$, $n = 11/11$) and mutant (J: $N = 2$, $n = 10/10$) 7 dpf retinas, revealing labeling of the apical Müller glia endfeet at the OLM (*arrows*) in both genotypes. **(K, L)** Labeling at the OLM (*arrows*) of F-actin (phalloidin) and Müller glia endfeet in a *Tg(gfap:egfp)* background in WT ($n = 7/7$) and *sema3fa^{ca304}* ($n = 8/8$) 15 dpf retinas. **(M, N)** Working model of roles for Sema3fa in regulating vascularization of the neural retina. Choroid vasculature **(M):** In WT, the choroid plexus (CP) remains outside of the RPE and Bruch's membrane (bm) through the release of Sema3fa (*purple hexagon*) by cells of the inner nuclear layer and the RPE. If Sema3fa signaling is perturbed, vessels pass through the RPE and leak into the nuclear layers containing the cone and rod (C/R) photoreceptors, horizontal cells (HC), and bipolar cells (BC). Hyaloid/retinal vasculature **(N):** Sema3fa (*purple hexagon*) maintains spacing and reduces the density of the blood vessel networks in WT retinas. In the absence of Sema3fa blood vessels overgrow. We propose that in both models Sema3fa acts via Nrp2b (*yellow rectangle*) and blood vessel growth is supported but not driven by the pro-angiogenic Vegf.

both these tissues, and the choroid vessels grow both precociously and inappropriately through the RPE and into the outer retina when the Sema3fa signal is absent (Fig. 6M). In the larval and adult retina, cells of the inner nuclear layer and CMZ, proximate to the hyaloid vasculature express Sem3fa (Fig. 6N). This expression is established at about 72 hpf, while the hyaloid vessel grows into the forming optic cup at 18 hpf, and a rudimentary vessel network is present by 2.5 dpf.[12] Thus it is not surprising that early hyaloid development occurs normally in *sema3fa* mutants. The hyaloid vessels normally refine into a simple hyaloid vasculature. In Sema3fa mutants, hyaloid vessels fail to refine, and the mature retinal vasculature network is more extensive than normal with the loss of Sema3fa (Fig. 6N). We propose that Sema3fa works in a direct paracrine manner on endothelial cells of the eye vasculature. In support, AAV-mediated

expression of SEMA3F in mouse models inhibits sprouting from retinal and choroidal vessels.[8,11] The fact that quantitatively similar phenotypes were observed in both heterozygotes and homozygotes suggests that Sema3fa is haploinsufficient, where even slightly lowered levels of Sema3fa results in aberrant vessel growth. VEGF-A is also known to be haploinsufficient,[47] indicating that fine-tuning of proangiogenic and antiangiogenic signals is critical for balancing growth and quiescence.

The initial analysis of the *Sema3f* null mouse did not report vascular abnormalities,[48] but based on our results further analysis is likely warranted. While our work in fish, and that with exogenous SEMA3F in mouse,[8,11] indicates that SEMA3F inhibits vessel growth for the eye, SEMA3F is a proangiogenic in the mouse placenta.[49,50] Thus SEMA3F may function in a tissue-specific manner, likely through different

combinations of receptors or downstream signaling components.

The *sema3fa* mutant vessel phenotypes could arise through a number of means, including increased endothelial cell proliferation, increased stability of vessels, or failure to block proangiogenic cellular guidance. VEGF might be important in this regard. VEGFA promotes endothelial cell proliferation[51–54] and contributes to pathologic neovascularization in the mouse retina.[55] We find that *vegfaa* and *vegfab* are expressed at similar levels in both WT and mutant larval retinas; however, arguing either that the normal physiological level of retinal VEGF is sufficient to "pull" choroidal vessels into the retina in the absence of the repulsive signal provided by Sema3fa, or that additional signals are upregulated in the absence of Sema3fa to promote vessel invasion (Fig. 6M). Interestingly, Sema3f signals through Nrp2 to inhibit VEGF-induced proliferation of endothelial cells of cultured human umbilical vein endothelial cells,[49] through competitive binding to the same receptor, suggesting that Sema3fa could limit choroid vessel sprouting in part by a block of VEGF-induced proliferation.

In mice and humans, choroidal vessels that invade the neural retina are generally immature and lack proper tight junctions between endothelial cells and smooth muscle/pericyte coverage and are therefore leakage prone.[56] Presumably the immaturity of the newly arrived vessels also explains the vascular leakage we observe in *sema3fa* mutants. In patients with wet AMD, leakage results in subsequent fluid accumulation in the macula of the retina that accelerates vision loss.[4] Interestingly, although we found nearly full penetrance of vascular leakage in *sema3fa* mutants, no obvious edema was present, nor did we find evidence of retinal detachments. Potentially, only the new vessels leak, and the regenerative capacity of zebrafish can correct any insult.

Glial cells are important in regulating the growth of eye blood vessels. Müller glia-derived VEGF contributes to pathologic neovascularization in the mouse retina,[55] and the retinal vasculature is thought to associate with an astrocyte scaffold that influences branching pattern in a VEGF-dependent manner in mammals.[57] Although no astrocytic scaffold has been identified in zebrafish, it is possible that Müller glia still play some role in vascular patterning in teleosts, in that the glial end feet form intimate connections with the endothelium after vascular dissection.[12] One interesting idea is that Müller glia, whose cell bodies reside in the inner nuclear layer, secrete Sema3fa preferentially from their end feet in contact with the inner limiting membrane and overlying endothelium. The Sema3f would provide an opposing mechanism to that of proangiogenic VEGF in patterning the retinal vasculature.

Here we provide evidence that Sema3fa establishes and maintains physiological avascularity of the zebrafish retina through the lifetime of the fish. A role for secreted Sema3s in mediating blood vessel dynamics is known.[58] To the best of our knowledge, however, we show for the first time that the loss of an anti-angiogenic molecular barrier makes the RPE receptive to blood vessel infiltration in the absence of any further insults. The robustness of the *sema3fa* mutant zebrafish model in mitigating eye vessel pathology argues convincingly for its continued use for understanding the underlying cellular and molecular events that control the growth of the vessel networks that support eye function.

References

1. Country MW. Retinal metabolism: a comparative look at energetics in the retina. *Brain Res*. 2017;1672:50–57.
2. Campochiaro PA. Molecular pathogenesis of retinal and choroidal vascular diseases. *Progr Retin Eye Res*. 2015;49:67–81.
3. Lim LS, Mitchell P, Seddon JM, Holz FG, Wong TY. Age-related macular degeneration. *Lancet*. 2012;379(9827): 1728–1738.
4. Saint-Geniez M, D'Amore PA. Development and pathology of the hyaloid, choroidal and retinal vasculature. 2004;48(8–9):1045–1058.
5. Baffi J, Byrnes G, Chan CC, Csaky KG. Choroidal neovascularization in the rat induced by adenovirus mediated expression of vascular endothelial growth factor. *Invest Ophthalmol Vis Sci*. 2000;41:3582–3589.
6. Spilsbury K, Garrett KL, Shen WY, Constable IJ, Rakoczy PE. Overexpression of vascular endothelial growth factor (VEGF) in the retinal pigment epithelium leads to the development of choroidal neovascularization. *Am J Pathol*. 2000;157:135–144.
7. Cui C, Lu H. Clinical observations on the use of new anti-VEGF drug, conbercept, in age-related macular degeneration therapy: a meta-analysis. *Clin Interv Aging*. 2017;13:51–62.
8. Buehler A, Sitaras N, Favret S, et al. Semaphorin 3F forms an anti-angiogenic barrier in outer retina. *FEBS Lett*. 2013;587:1650–1655.
9. Barcelona PF, Sitaras N, Galan A, et al. p75NTR and Its ligand ProNGF activate paracrine mechanisms etiological to the vascular, inflammatory, and neurodegenerative pathologies of diabetic retinopathy. *J Neurosci*. 2016;36:8826–8841.
10. Fukushima Y, Okada M, Kataoka H, et al. Sema3E-PlexinD1 signaling selectively suppresses disoriented angiogenesis in ischemic retinopathy in mice. *J Clin Invest*. 2011;121:1974–1985.
11. Sun Y, Liegl R, Gong Y, et al. Sema3f Protects Against Subretinal Neovascularization In Vivo. *EBioMedicine*. 2017;18:281–287.
12. Alvarez Y, Cederlund ML, Cottell DC, et al. Genetic determinants of hyaloid and retinal vasculature in zebrafish. *BMC Dev Bio*. 2007;7:114.
13. Fruttiger M. Development of the retinal vasculature. *Angiogenesis*. 2007;10:77–88.
14. Provis JM. Development of the primate retinal vasculature. *Prog Retin Eye Res*. 2001;20:799–821.
15. Hwang WY, Fu Y, Reyon D, et al. Efficient genome editing in zebrafish using a CRISPR-Cas system. *Nat Biotechnol*. 2013;31:227–229.
16. Fishman MC, Chien KR. Fashioning the vertebrate heart: earliest embryonic decisions. *Development*. 1997;124:2099–2117.

17. Kimmel CB, Ballard WW, Kimmel SR, Ullmann B, Schilling TF. Stages of embryonic development of the zebrafish. *Dev Dyn.* 1995;203:253–310.

18. Montague TG, Cruz JM, Gagnon JA, Church GM, Valen E. CHOPCHOP: a CRISPR/Cas9 and TALEN web tool for genome editing. *Nuc Acids Res.* 2014;42:W401–W407.

19. Meeker ND, Hutchinson SA, Ho L, Trede NS. Method for isolation of PCR-ready genomic DNA from zebrafish tissues. *Biotechniques.* 2007;43:610, 612, 614.

20. Proulx K, Lu A, Sumanas S. Cranial vasculature in zebrafish forms by angioblast cluster-derived angiogenesis. *Dev Biol.* 2010;348:34–46.

21. Peterson SM, Freeman JL. RNA isolation from embryonic zebrafish and cDNA synthesis for gene expression analysis. *J Vis Exp.* 2009;(30):1470.

22. Thisse C, Thisse B. High-resolution in situ hybridization to whole–mount zebrafish embryos. *Nat Protoc.* 2008;3:59–69.

23. Childs S, Chen J-N, Garrity DM, Fishman MC. Patterning of angiogenesis in the zebrafish embryo. *Development.* 2002;129:973–982.

24. Sullivan-Brown J, Bisher ME, Burdine RD. Embedding, serial sectioning and staining of zebrafish embryos using JB-4 resin. *Nat Protoc.* 2011;6:46–55.

25. Raymond PA, Colvin SM, Jabeen Z, et al. Patterning the cone mosaic array in zebrafish retina requires specification of ultraviolet-sensitive cones. *PLoS ONE.* 2014;9:e85325.

26. Bozic I, Li X, Tao Y. Quantitative biometry of zebrafish retinal vasculature using optical coherence tomographic angiography. *Biomed Opt Express.* 2018;9:1244–1255.

27. Cao R, Jensen LDE, Söll I, Hauptmann G, Cao Y. Hypoxia-induced retinal angiogenesis in zebrafish as a model to study retinopathy. *PLoS ONE.* 2008;3:e2748.

28. Leung YF, Ma P, Dowling JE. Gene expression profiling of zebrafish embryonic retinal pigment epithelium in vivo. *Invest Ophthalmol Vis Sci.* 2007;48:881–890.

29. Chen H, He Z, Bagri A, Tessier-Lavigne M. Semaphorin-neuropilin interactions underlying sympathetic axon responses to class III semaphorins. *Neuron.* 1998;21:1283–1290.

30. Kolodkin AL, Levengood DV, Rowe EG, Tai YT, Giger RJ, Ginty DD. Neuropilin is a semaphorin III receptor. *Cell.* 1997;90:753–762.

31. Giger RJ, Cloutier JF, Sahay A, et al. Neuropilin-2 is required in vivo for selective axon guidance responses to secreted semaphorins. *Neuron.* 2000;25:29–41.

32. Tamagnone L, Artigiani S, Chen H, et al. Plexins are a large family of receptors for transmembrane, secreted, and GPI-anchored semaphorins in vertebrates. *Cell.* 1999;99:71–80.

33. Hartsock A, Lee C, Arnold V, Gross JM. In vivo analysis of hyaloid vasculature morphogenesis in zebrafish: A role for the lens in maturation and maintenance of the hyaloid. *Dev Biol.* 2014;394:327–339.

34. Isogai S, Horiguchi M, Weinstein BM. The vascular anatomy of the developing zebrafish: an atlas of embryonic and early larval development. *Dev Biol.* 2001;230:278–301.

35. Hashiura T, Kimura E, Fujisawa S, et al. Live imaging of primary ocular vasculature formation in zebrafish. *PLoS One.* 2017;12(4):e0176456.

36. van Rooijen E, Voest EE, Logister I, et al. von Hippel-Lindau tumor suppressor mutants faithfully model pathological hypoxia-driven angiogenesis and vascular retinopathies in zebrafish. *Dis Model Mech.* 2010;3(5–6):343–353.

37. Cheung N, Wong IY, Wong TY. Ocular anti-VEGF therapy for diabetic retinopathy: overview of clinical efficacy and evolving applications. *Diabetes Care.* 2014;37:900–905.

38. Coultas L, Chawengsaksophak K, Rossant J. Endothelial cells and VEGF in vascular development. *Nature.* 2005;438:937–945.

39. Bahary N, Goishi K, Stuckenholz C, et al. Duplicate VegfA genes and orthologues of the KDR receptor tyrosine kinase family mediate vascular development in the zebrafish. *Blood.* 2007;110:3627–3636.

40. Schultz LE, Solin SL, Wierson WA, et al. Vascular endothelial growth factor a and leptin expression associated with ectopic proliferation and retinal dysplasia in zebrafish optic pathway tumors. *Zebrafish.* 2017;14:343–356.

41. Ersoz MG, Karacorlu M, Arf S, Sayman Muslubas I, Hocaoglu M. Retinal pigment epithelium tears: classification, pathogenesis, predictors, and management. *Surv Ophthalmol.* 2017;62:493–505.

42. Zou J, Lathrop KL, Sun M, Wei X. Intact retinal pigment epithelium maintained by Nok is essential for retinal epithelial polarity and cellular patterning in zebrafish. *J Neurosci.* 2008;28:13684–13695.

43. Omri S, Omri B, Savoldelli M, et al. The outer limiting membrane (OLM) revisited: clinical implications. *Clin Ophthalmol.* 2010;4:183–195.

44. Kujawski S, Sonawane M, Knust E. penner/lgl2 is required for the integrity of the photoreceptor layer in the zebrafish retina. *Biol Open.* 2019;8(4):bio041830.

45. Biehlmaier O, Neuhauss SCF, Kohler K. Double cone dystrophy and RPE degeneration in the retina of the zebrafish gnn mutant. *Invest Ophthalmol Vis Sci.* 2003;44:1287–1298.

46. Krock BL, Perkins BD. The Par-PrkC polarity complex is required for cilia growth in zebrafish photoreceptors. *PLoS ONE.* 2014;9(8):e104661.

47. Ferrara N, Carver-Moore K, Chen H, et al. Heterozygous embryonic lethality induced by targeted inactivation of the VEGF gene. *Nature.* 1996;380:439–442.

48. Sahay A, Molliver ME, Ginty DD, Kolodkin AL. Semaphorin 3F is critical for development of limbic system circuitry and is required in neurons for selective CNS axon guidance events. *J Neurosci.* 2003;23:6671–6680.

49. Kessler O, Shraga-Heled N, Lange T, et al. Semaphorin-3F is an inhibitor of tumor angiogenesis. *Cancer Res.* 2004;64:1008–1015.

50. Regano D, Visintin A, Clapero F, et al. Sema3F (Semaphorin 3F) selectively drives an extraembryonic proangiogenic program. *Arterioscler Thromb Vasc Biol.* 2017;37:1710–1721.

51. Mahabeleshwar GH, Feng W, Reddy K, Plow EF, Byzova TV. Mechanisms of integrin-vascular endothelial growth factor receptor cross-activation in angiogenesis. *Circ Res.* 2007;101:570–580.

52. Soldi R, Mitola S, Strasly M, Defilippi P, Tarone G, Bussolino F. Role of $\alpha(v)\beta3$ integrin in the activation of vascular endothelial growth factor receptor-2. *EMBO J.* 1999;18:882–892.

53. Werdich XQ, Penn JS. Src, Fyn and Yes play differential roles in VEGF-mediated endothelial cell events. *Angiogenesis.* 2005;8:315–326.

54. West XZ, Meller N, Malinin NL, et al. Integrin β 3 crosstalk with VEGFR accommodating tyrosine phosphorylation as a regulatory switch. *PLoS ONE.* 2012;7(2):e31071.

55. Bai Y, Ma JX, Guo J, et al. Müller cell-derived VEGF is a significant contributor to retinal neovascularization. *J Pathol.* 2009;219:446–454.

56. Törnquist P, Alm A, Bill A. Permeability of ocular vessels and transport across the blood-retinal-barrier. *Eye (Lond).* 1990;4(Pt 2):303–309.

57. Gerhardt H, Golding M, Fruttiger M, et al. VEGF guides angiogenic sprouting utilizing endothelial tip cell filopodia. *J Cell Biol.* 2003;161:1163–1177.

58. Sakurai A, Doci C, Gutkind JS. Semaphorin signaling in angiogenesis, lymphangiogenesis and cancer. *Cell Res.* 2012;22:23–32.